Spatially Variant Morphological Restoration and Skeleton Representation

Nidhal Bouaynaya, *Student Member, IEEE*, Mohammed Charif-Chefchaouni, and Dan Schonfeld, *Senior Member, IEEE*

***Abstract*—The theory of spatially variant (SV) mathematical morphology is used to extend and analyze two important image processing applications: morphological image restoration and skeleton representation of binary images. For morphological image restoration, we propose the SV alternating sequential filters and SV median filters. We establish the relation of SV median filters to the basic SV morphological operators (i.e., SV erosions and SV dilations). For skeleton representation, we present a general framework for the SV morphological skeleton representation of binary images. We study the properties of the SV morphological skeleton representation and derive conditions for its invertibility. We also develop an algorithm for the implementation of the SV morphological skeleton representation of binary images. The latter algorithm is based on the optimal construction of the SV structuring element mapping designed to minimize the cardinality of the SV morphological skeleton representation. Experimental results show the dramatic improvement in the performance of the SV morphological restoration and SV morphological skeleton representation algorithms in comparison to their translation-invariant counterparts.**

***Index Terms*—Adaptive morphology, alternating sequential filter, kernel representation, median filter, morphological skeleton representation, spatially variant mathematical morphology.**

I. Introduction

OVER the past few decades, morphological operators have gained increasing popularity in the implementation of signal and image processing systems [1]–[12]. The inherent parallelism of the class of morphological filters allows the implementation of very efficient and low-complexity algorithms for signal and image processing applications [1], [2], [6], [9]–[11], [13]–[16].

The basic concepts and analytic tools in mathematical morphology can be found, for binary images, in set theory and integral geometry [6], [9]. In mathematical morphology, a binary image is represented as a subset of the two-dimensional (2–D) Euclidean space, $\mathbb{R}^2$ or its digitized equivalent $\mathbb{Z}^2$, and image processing transformations are represented as set mappings between collections of subsets. Erosions and dilations are the two fundamental morphological operators [1], [2], [17]–[21]. They are characterized by a subset called the structuring element that is used to probe the image. Matheron has captured the ubiquity of morphological operators by demonstrating that any increasing (i.e., operators which preserve signal ordering) and translation-invariant operators can be represented as unions (respectively, intersections) of erosions (respectively, dilations) [6].

In most applications of mathematical morphology, the structuring element remains constant in shape and size as the image is probed. Hence, the focus of mathematical morphology has been mostly devoted to translation-invariant operators. An extension of the theory to spatially variant (SV) operators has emerged due to the requirements of some applications, such as traffic spatial measurements [22] and range imagery [23]. For example, in the analysis of images from traffic control cameras in [11], vehicles at the bottom of the image are closer and appear larger than those higher in the image. Hence, the structuring element size should vary linearly with the vertical position in the image. In range imagery, the value of each pixel is related to the distance to the imaging device. Consequently, the apparent height of an object is a function of the object's intensity range. Hence, one can process (e.g., extract or eliminate) differently scaled objects of interest in the image by adapting the size of the structuring element(s) to the local intensity range [23].

Different techniques and algorithms to spatially adapt the structuring element in an image have been proposed in [23]–[28]. Roerdink [29], [30] introduced the theoretical background for a mathematical morphology that is not based on translation-invariant transformations in the Euclidean space. The proposed approach, however, is restricted by various rigid algebraic constructions such as polar morphology and constrained perspective morphology. In [31], a new class of morphological operations, which allow one to select varying shapes and orientations of structuring elements, is presented. However, the sweep erosion and dilation do not satisfy the basic properties of mathematical morphology. In particular, they are not increasing operators in general and the sweep dilation operator does not commute with the union. A unified theory of SV mathematical morphology requires a further abstraction of the basic notions of translation-invariant mathematical morphology. A fundamental result in lattice morphology[1] that provides the representation of a large class of nonlinear and nonnecessarily translation-invariant operators in terms of lattice erosions and dilations has been presented in [33]. This

Manuscript received June 3, 2005; revised January 5, 2006. The associate editor coordinating the review of this manuscript and approving it for publication was Dr. Giovanni Ramponi.

N. Bouaynaya and D. Schonfeld are with the Department of Electrical and Computer Engineering, University of Illinois at Chicago, Chicago, IL 60607 USA (e-mail: nbouay1@uic.edu, ds@ece.uic.edu).

M. Charif-Chefchaouni is with the Institut National des Postes et Télécommunications, Rabat, Morocco (e-mail: charifm@inpt.ac.ma).

Digital Object Identifier 10.1109/TIP.2006.877475

[1]Lattice morphology, introduced by Serra [11], is a powerful tool for the abstraction of mathematical morphology based on lattice theory, a topic devoted to the investigation of the algebraic properties of partially ordered sets [32].

representation, however, does not posses the geometric interpretation, captured by the structuring element, that is crucial in signal and image processing. A separate approach to the representation of SV mathematical morphology, which preserves the geometrical structuring element, in the Euclidean space, has been introduced by Serra in [11]. Serra defined the concept of a structuring function, which associates to each point in the space a structuring element. Charif-Chefchaouni and Schonfeld [34], [35] pursued the investigation of SV mathematical morphology in a systematic way. They introduced the basic SV morphological operators and investigated their properties. A comprehensive development of the theory of SV mathematical morphology in the Euclidean space has been presented in [36].

This paper elaborates on the theory and applications of SV mathematical morphology presented in [36]. We illustrate the power of the theory of SV mathematical morphology for two important image processing applications: morphological image restoration and skeleton representation.

Morphological Image restoration is an important problem in image processing and analysis applications. It requires the development of an efficient filtering procedure which restores an image from its noisy version [4], [5], [8], [11], [37], [38]. In order to devise such a filtering procedure, we have to consider two fundamental issues: 1) the restoration filter should be effective in eliminating the noise degradation and 2) it should be able to restore various important aspects of the shape-size content of the noise-free image under consideration, as well as preserve its crucial geometrical and topological structure. The effectiveness of morphological filters in the restoration of noisy images has been demonstrated repeatedly [4], [8], [9], [11], [22], [37]–[41]. For example, Maragos and Schafer [4] have demonstrated a strong relationship between the alternating filter and the median filter. Sternberg [37] introduced alternating sequential filters (ASF) and experimentally showed their noise removal capability. Moreover, Schonfeld and Goutsias [8] have shown that the class of alternating sequential filters is a set of smoothing morphological filters which best preserve the crucial structure of input images, in the least-mean-difference sense. Translation-invariant morphological filters can be used to remove noise structures that are smaller than the size of the structuring element. However, some important features of the signal might be removed as well. Many researchers considered adaptive morphological filtering in order to deal with this problem [24]–[26]. For example, Chen *et al.* [24], developed an algorithm for adaptive signal smoothing by spatially varying the filtering scales depending on the local property of each point in the signal. To achieve this goal, they introduced the progressive umbra-filling (PUF) procedure. Their experimental results have shown that this approach can successfully eliminate noise without oversmoothing the important features of a signal. It can be easily established that the morphological operators proposed in [24] are the gray-level extensions of the SV binary morphological operators [42]. In this paper, we show that the theory of SV mathematical morphology unifies many classical morphological filters that use SV structuring elements, which are suitable for adaptive image processing applications. We introduce SV alternating sequential filters and SV median filters for the restoration of images from their noisy versions. We derive the basic properties of SV alternating sequential filters. We also derive a kernel representation of SV median filters, which establishes the relation between the SV median filters and the basic SV morphological operators.

We also demonstrate the power of the theory of SV mathematical morphology by generalizing the morphological skeleton representation to the SV morphological skeleton representation. The morphological skeleton has been investigated by many researchers [9], [43]–[46], mainly for the purpose of image coding and shape recognition. In [44], a general theory for the morphological representation of discrete binary images was presented. The basis of this theory relies upon the generation of a set of nonoverlapping segments of an image, which produce a decomposition that guarantees exact reconstruction of the original image. Decreasing the cardinality of the morphological skeleton representation by reducing its redundancy has been explored by many authors [43], [44], [46]. In this paper, We extend the morphological skeleton representation framework presented in [44] to the SV case. We study the properties of the SV morphological skeleton representation and derive conditions for its invertibility. We also propose an algorithm for the implementation of the SV morphological skeleton. This algorithm minimizes the cardinality of the image representation by deriving an optimal universal algorithm for the construction of a SV structuring element mapping.

This paper is organized as follows. In Section II, we provide a brief overview of SV mathematical morphology. Specifically, we present the basic SV morphological operators. We summarize the SV kernel representation, which shows that any increasing operator that fixes the entire space can be represented as a union (respectively, intersection) of SV erosions (respectively, SV dilations). This result demonstrates the ubiquity of the basic SV morphological operators (i.e., SV erosions and SV dilations). In Section III, we illustrate the impact of SV mathematical morphology on image restoration applications. In particular, we address morphological image restoration by introducing the SV alternating sequential filters and SV median filters. We also provide an example for selection of the SV structuring element mapping for image restoration applications. We experimentally show the superior noise removal capabilities of these filters compared to their translation-invariant counterparts. In Section IV, we demonstrate the power of SV mathematical morphology in skeleton representation applications. Specifically, we propose the SV morphological skeleton representation, develop some of its properties and derive conditions for its invertibility. We further propose a universal algorithm for the implementation of the SV morphological skeleton representation. We provide simulation results which demonstrate the enormous improvement of the SV morphological skeleton representation in comparison to its translation-invariant counterpart. Finally, in Section V, we present a brief summary of our results and discuss our plan for future work.

The proofs of all theoretical results that are new contributions in this paper are presented in Appendices A and B.

II. Spatially Variant Mathematical Morphology

Notation: We consider a nonempty set $\xi = \mathbb{R}^n$ or $\mathbb{Z}^n$. The set $\mathcal{P}(\xi)$ denotes the set of all subsets of ξ. Elements of the set ξ

will be denoted by lower-case letters; e.g., a, b, c. Elements of the set $\mathcal{P}(\xi)$ will be denoted by upper-case letters; e.g., A, B, C. An order on $\mathcal{P}(\xi)$ is imposed by the inclusion $\subseteq$. We use $\cup$ and $\cap$ to denote the union and intersection in $\mathcal{P}(\xi)$, respectively. X^c denotes the complement of $X \in \mathcal{P}(\xi)$. The set difference $X_1 - X_2$ of sets X_1 and X_2 is defined by $X_1 - X_2 = X_1 \cap X_2^c$. The translation $X + \{y\}$ also denoted by X_y of a set $X \in \mathcal{P}(\xi)$ by $y \in \xi$ is defined by $X + \{y\} = X_y = \{z : z = x + y,\ x \in X\}$. The cardinality $|X|$ of a set X is the total number of elements contained in the set. We use $\mathcal{O} = \mathcal{P}(\xi)^{\mathcal{P}(\xi)}$ to denote the set of all operators mapping $\mathcal{P}(\xi)$ into itself. Elements of the set $\mathcal{O}$ will be denoted by lower case Greek letters; e.g., α, β, γ. An order on $\mathcal{O}$ is imposed by the inclusion $\subseteq$; i.e., $\alpha \subseteq \beta$ if and only if $\alpha(X) \subseteq \beta(X)$, for every $X \in \mathcal{P}(\xi)$. We shall restrict our attention to nondegenerate operators; i.e., $\alpha(X) \neq \xi$ and $\alpha(X) \neq \emptyset$ for some $X \in \mathcal{P}(\xi)$ and $\alpha(\emptyset) = \emptyset$, for every $\alpha \in \mathcal{O}$ (the set $\emptyset \in \mathcal{P}(\xi)$ is used to denote the empty set).

A mapping $\psi \in \mathcal{O}$ is:

- *increasing* if $X \subseteq Y \Longrightarrow \psi(X) \subseteq \psi(Y)$, for all $X, Y \in \mathcal{P}(\xi)$;
- *translation-invariant* if $\psi(X_a) = (\psi(X))_a$, for every $X \in \mathcal{P}(\xi)$ and every $a \in \xi$;
- *extensive* (respectively, *anti-extensive*) if $X \subseteq \psi(X)$ (respectively, $\psi(X) \subseteq X$), for all $X \in \mathcal{P}(\xi)$;
- *idempotent* if $\psi(\psi(X)) = \psi(X)$, for all $X \in \mathcal{P}(\xi)$.

The mapping $\psi^* \in \mathcal{O}$ is the dual of the mapping $\psi \in \mathcal{O}$ iff

$$\psi^*(X) = (\psi(X^c))^c \quad (X \in \mathcal{P}(\xi)).$$

A. SV Morphological Operators

We shall now present an overview of the basic definitions and properties of SV mathematical morphology introduced by Charif-Chefchaouni and Schonfeld [34], [35]. For a more comprehensive introduction to SV mathematical morphology refer to [36].[2]

1) SV Erosions and SV Dilations: The SV structuring element θ is a mapping from ξ into $\mathcal{P}(\xi)$. The transposed SV structuring element θ' is a mapping from ξ into $\mathcal{P}(\xi)$ given by

$$\theta'(y) = \{z \in \xi : y \in \theta(z)\} \quad (y \in \xi). \tag{1}$$

In translation-invariant mathematical morphology, θ is the translation mapping by a fixed set $B \in \mathcal{P}(\xi)$, i.e., $\theta(z) = B + z$, $z \in \xi$. Hence, the transposed structuring element corresponds to the translation by the transposed set $\check{B} = \{-b : b \in B\}$.

The SV erosion $\mathcal{E}_\theta \in \mathcal{O}$ is given by

$$\mathcal{E}_\theta(X) = \{z \in \xi : \theta(z) \subseteq X\} = \bigcap_{y \in X^c} \theta'^c(y) \quad (X \in \mathcal{P}(\xi)). \tag{2}$$

[2]Some of the results presented in this section have been extended to the gray-level case by Chen *et al.* [24], [25].

The SV dilation $\mathcal{D}_\theta \in \mathcal{O}$ is given by

$$\mathcal{D}_\theta(X) = \{z \in \xi : \theta(z) \cap X \neq \emptyset\} = \bigcup_{y \in X} \theta'(y) \quad (X \in \mathcal{P}(\xi)). \tag{3}$$

The SV erosions and dilations satisfy the basic properties of translation-invariant erosions and dilations. Below we list the main properties that we need in the sequel.

2) Properties of SV Erosions and SV Dilations:

a) *Adjunction*: For every mapping θ from ξ to $\mathcal{P}(\xi)$ the pair $(\mathcal{E}_\theta, \mathcal{D}_{\theta'})$ defines an adjunction on $\mathcal{P}(\xi)$. In other words

$$\mathcal{D}_\theta(X) \subseteq Y \Longleftrightarrow X \subseteq \mathcal{E}_{\theta'}(Y) \quad (X, Y \in \mathcal{P}(\xi)). \tag{4}$$

This result states that $\mathcal{E}_\theta$ and $\mathcal{D}_\theta$ are an erosion and a dilation, respectively, in the sense that these operators are distributive over intersection and union, respectively, i.e.,

$$\mathcal{E}_\theta\left(\bigcap_{i \in I} X_i\right) = \bigcap_{i \in I} \mathcal{E}_\theta(X_i), \text{ and } \mathcal{D}_\theta\left(\bigcup_{i \in I} X_i\right) = \bigcup_{i \in I} \mathcal{D}_\theta(X_i) \tag{5}$$

for an arbitrary collection of sets $\{X_i \in \mathcal{P}(\xi) : i \in I\}$. These identities can also be derived easily without reference to the framework of adjunctions.

b) *Duality*: The SV erosion $\mathcal{E}_\theta$ and the SV dilation $\mathcal{D}_\theta$ are dual operators, i.e.,

$$\mathcal{E}_\theta{}^*(X) = \mathcal{D}_\theta(X) \quad (X \in \mathcal{P}(\xi)). \tag{6}$$

This relation states that dilating a set X by the mapping θ is equivalent to eroding its complement X^c by the same mapping and complementing the result.

c) *Increasing*: For a given mapping θ, the SV erosion $\mathcal{E}_\theta$ and the SV dilation $\mathcal{D}_\theta$ are increasing operators, i.e.,

$$X \subseteq Y \Longrightarrow \mathcal{E}_\theta(X) \subseteq \mathcal{E}_\theta(Y), \text{ and } \mathcal{D}_\theta(X) \subseteq \mathcal{D}_\theta(Y). \tag{7}$$

Increasing operators preserve order (contrast) in the sense that they prohibit extraction of information from occluded regions. This property is consistent with the models of the human visual system which have been investigated in the field of cognitive psychology. Specifically, the high-level vision models of gestalt psychology state that the perceptual processes underlying the visual interpretation of a scene are increasing operators [9], [47], [48].

d) *Extensivity and Anti-Extensivity*: If $z \in \theta(z)$ for every $z \in \xi$, then the SV erosion $\mathcal{E}_\theta$ is anti-extensive and the SV dilation $\mathcal{D}_\theta$ is extensive, i.e.,

$$\mathcal{E}_\theta(X) \subseteq X, \text{ and } X \subseteq \mathcal{D}_\theta(X) \quad (X \in \mathcal{P}(\xi)). \tag{8}$$

e) *Serial Composition*: Let us use $\mathcal{E}_{\theta_1}(\theta_2)$ and $\mathcal{D}_{\theta_1}(\theta_2)$ to denote the mappings from ξ into $\mathcal{P}(\xi)$ given by $(\mathcal{E}_{\theta_1}(\theta_2))(z) = \mathcal{E}_{\theta_1}(\theta_2(z))$ and $(\mathcal{D}_{\theta_1}(\theta_2))(z) = \mathcal{D}_{\theta_1}(\theta_2(z))$, for every $z \in \xi$. Successively SV eroding (respectively, SV dilating) a set first by θ_1 and then by θ_2 is equivalent to SV eroding (respectively, SV dilating) by the dilated mapping $\mathcal{D}_{\theta_1'}(\theta_2)$, i.e., we have

$$\mathcal{E}_{\theta_2}(\mathcal{E}_{\theta_1}(X)) = \mathcal{E}_{\mathcal{D}_{\theta_1'}}(\theta_2)(X) \quad (X \in \mathcal{P}(\xi)) \tag{9}$$

and

$$\mathcal{D}_{\theta_2}(\mathcal{D}_{\theta_1}(X)) = \mathcal{D}_{\mathcal{D}_{\theta_1'}(\theta_2)}(X) \quad (X \in \mathcal{P}(\xi)). \tag{10}$$

3) SV Openings and SV Closings: We shall now present the SV openings and closings and review their main properties. The SV opening $\Gamma_\theta \in \mathcal{O}$ is given by

$$\Gamma_\theta(X) = \mathcal{D}_{\theta'}(\mathcal{E}_\theta(X)) \quad (X \in \mathcal{P}(\xi)). \tag{11}$$

The SV closing $\Phi_\theta \in \mathcal{O}$ is given by

$$\Phi_\theta(X) = \mathcal{E}_{\theta'}(\mathcal{D}_\theta(X)) \quad (X \in \mathcal{P}(\xi)). \tag{12}$$

The SV opening and SV closing have nice geometrical interpretations. Let us refer to $\theta(z)$ by the *local structuring element* at point z. The SV opening of a set X is the domain swept out by all local structuring elements which are included in X. By duality, a point z belongs to the SV closing if and only if all the local structuring elements containing z hit X. Formally, we have the following equivalent definitions for the SV opening and SV closing:

$$\Gamma_\theta(X) = \bigcup\{\theta(y) : \theta(y) \subseteq X; y \in \xi\} \tag{13}$$

$$\Phi_\theta(X) = \{z \in \xi : \theta(y) \cap X \neq 0, \text{ for every } \theta(y) : z \in \theta(y)\} \tag{14}$$

for every $X \in \mathcal{P}(\xi)$.

4) Properties of SV Openings and SV Closings:

a) *Duality*: The SV opening Γ_θ and the SV closing Φ_θ are dual operators, i.e.,

$$\Gamma_\theta^*(X) = \Phi_\theta(X) \quad (X \in \mathcal{P}(\xi)). \tag{15}$$

b) *Increasing*: For a given θ, the SV opening Γ_θ and the SV closing Φ_θ are increasing operators on $\mathcal{P}(\xi)$, i.e.,

$$X \subseteq Y \Longrightarrow \Gamma_\theta(X) \subseteq \Gamma_\theta(Y), \text{ and } \Phi_\theta(X) \subseteq \Phi_\theta(Y). \tag{16}$$

c) *Extensivity and Anti-Extensivity*: For every mapping θ, the SV opening (respectively, SV closing) is anti-extensive (respectively, extensive). We have

$$\Gamma_\theta(X) \subseteq X, \text{ and } \Phi_\theta(X) \supseteq X \quad (X \in \mathcal{P}(\xi)). \tag{17}$$

d) *Idempotence*: The SV opening Γ_θ and SV closing Φ_θ are idempotent operators, i.e., for every $X \in \mathcal{P}(\xi)$,

$$\Gamma_\theta(\Gamma_\theta(X)) = \Gamma_\theta(X) \text{ and } \Phi_\theta(\Phi_\theta(X)) = \Phi_\theta(X). \tag{18}$$

e) *Fixed Points*: It was shown in [6] and [49] that the translation-invariant opening and closing can be completely specified from their fixed points. The framework of fixed points can be extended to the SV case by defining θ-open and θ-closed sets as follows.

5) Definition 1: $X \in \mathcal{P}(\xi)$ is θ-open (respectively, θ-closed) if $\Gamma_\theta(X) = X$ [respectively, $\Phi_\theta(X) = X$].

A useful characterization of θ-open and θ-closed sets is given by the following proposition.

Proposition 1: [36] $X \in \mathcal{P}(\xi)$ is θ-open [respectively, θ-closed] if and only if there exists $Y \in \mathcal{P}(\xi)$ such that $X = \mathcal{D}_{\theta'}(Y)$ (respectively, $X = \mathcal{E}_{\theta'}(Y)$).

The concept of θ-open and θ-closed sets was further extended to mappings as follows. Consider mappings θ_1 and θ_2 from ξ into $\mathcal{P}(\xi)$. The mapping θ_1 is θ_2-open (respectively, θ_2 closed) if $\theta_1(z)$ is θ_2-open (respectively, θ_2-closed), for every $z \in \xi$. We then have the following result: If θ_1 is θ_2-open, then

$$\Gamma_{\theta_1}(X) \subseteq \Gamma_{\theta_2}(X), \text{ and } \Phi_{\theta_2}(X) \subseteq \Phi_{\theta_1}(x) \quad (X \in \mathcal{P}(\xi)). \tag{19}$$

a) *Sieving structure*: If θ_1 is θ_2 open, then we have

$$\Gamma_{\theta_1}(\Gamma_{\theta_2}(X)) = \Gamma_{\theta_1}(X); \quad \Gamma_{\theta_2}(\Gamma_{\theta_1}(X)) = \Gamma_{\theta_1}(X) \tag{20}$$

and

$$\Phi_{\theta_1}(\Phi_{\theta_2}(X)) = \Phi_{\theta_1}(X); \quad \Phi_{\theta_2}(\Phi_{\theta_1}(X)) = \Phi_{\theta_1}(X) \tag{21}$$

for every $X \in \mathcal{P}(\xi)$.

B. SV Kernel Representation

An important notion related to set mappings is that of the kernel, introduced by Matheron [6] for translation-invariant mappings. Matheron subsequently showed that every increasing and translation-invariant operator can be written as a union of translation-invariant erosions, or, alternatively, as an intersection of translation-invariant dilations. This result was extended to SV operators in [36]. To state the corresponding theorem, we need the notion of a SV kernel. Let $\psi \in \mathcal{O}$. The SV kernel $Ker(\psi)$ of ψ is given by

$$Ker(\psi) = \{\theta : z \in \psi(\theta(z)) \text{ for every } z \in \xi\}. \tag{22}$$

An operator $\psi \in \mathcal{O}$ is a covering operator (abbreviated as $\mathcal{C}$-operator) if ψ is increasing and satisfies $\psi(\xi) = \xi$. An important property of $\mathcal{C}$-operators is that their kernel is nontrivial and is unique. In other words, the mapping which associates to each $\mathcal{C}$-operator its kernel is a one-to-one mapping. [36].

The kernel representation of $\mathcal{C}$-operators is given by the following theorem;

Theorem 1: [36] An operator $\psi \in \mathcal{O}$ is a $\mathcal{C}$-operator if and only if

$$\psi(X) = \bigcup_{\theta \in Ker\ (\psi)} \mathcal{E}_\theta(X) = \bigcap_{\theta \in Ker\ (\psi^*)} \mathcal{D}_\theta(X) \tag{23}$$

for every $X \in \mathcal{P}(\xi)$.

Theorem 1 is not only interesting theoretically but also for practical applications. For some $\mathcal{C}$-operators, a subset of the kernel, called a basis, is sufficient for its representation in terms of SV erosions or SV dilations. Therefore, if the kernel of a $\mathcal{C}$-operator or one of its basis has a finite number of mappings then the $\mathcal{C}$-operator can be exactly represented as a finite union of SV erosions, or equivalently, as a finite intersection of SV dilations. This representation can tremendously simplify the analysis and implementation of the nonlinear $\mathcal{C}$-operator. We will show later that the adaptive median filter has a finite basis representation. Hence, it can be exactly expressed via a closed formula involving only intersections and unions of sets without requiring any sorting.

In Sections III–V, we apply the general theory of SV mathematical morphology to two image processing applications: morphological restoration of noisy images and morphological skeleton representation.

III. Spatially Variant Morphological Restoration

We shall consider SV alternating sequential filters (SVASF) and adaptive median filters for SV or adaptive image restoration.

A. SVASFs

1) Theoretical Aspects: Alternating sequential filters (ASFs) were introduced by Sternberg [37] and were extensively studied by Serra [11]. Basically, an alternating sequential filter is a composition of openings and closings by structuring elements of increasing sizes. In this section, we shall extend the class of ASF to the SV case. In our work $A \ominus B$ and $A \oplus B$ denote the translation-invariant erosion and dilation, respectively, between the sets A and $B \in \mathcal{P}(\xi)$. We use AF and ASF to denote the translation-invariant alternating filter and translation-invariant alternating sequential filter, respectively. SVAF and SVASF will denote the SVAF and SVASF, respectively.

Given a binary image X, let us assume that the transformation $\Theta(\bullet)$ produces a degraded binary image Y given by

$$Y = \Theta(X) = (X - N_1) \cup N_2 \tag{24}$$

where

$$N_i = \bigcup_{n=1,2,\ldots} C_{i,n} + \{x_{i,n}\}, \quad i = 1,2. \tag{25}$$

The model given by (25) is known as the *germ-grain model* [8], [9], [50]. In this case $\{C_{i,n}, n = 1,2,\ldots\}$ is a sequence of sets, known as the primary grains, whereas $\{x_{i,n}, n = 1,2,\ldots\}$ is a sequence of sites, known as the germs, which are randomly distributed in $\mathbb{Z}^2$; e.g., a Bernouilli point process.[3] Observe that the sequence of germs $\{x_{i,n}, n = 1,2,\ldots\}$ indicates the "centers" of the primary grains $\{C_{i,n}, n = 1,2,\ldots\}$ in the noise process N_i, $i = 1,2$.

The SVAF by the structuring element mapping θ is defined as the compound SV open-close

$$\mathrm{SVAF}_\theta(X) = \Phi_\theta(\Gamma_\theta(X)) \quad (X \in \mathcal{P}(\xi)). \tag{26}$$

A SV alternating sequential filter is an iterative application of SV alternating filters

$$\mathrm{SVASF}_N(X) = \mathrm{SVAF}_{\theta_N}\mathrm{SVAF}_{\theta_{N-1}} \cdots \mathrm{SVAF}_{\theta_1}(X) \tag{27}$$

where $X \in \mathcal{P}(\xi)$, $N \in \mathbb{N}^*$ is the order of the filter and the sequence $\{\theta_i\}_{i=1}^N$ is increasing i.e., $\theta_i(z) \subseteq \theta_{i+1}(z)$, for all $z \in \xi$, for all $1 \le i \le N-1$.

An operator $\psi \in \mathcal{O}$ is called a *morphological filter* if it is increasing and idempotent. This terminology is different from the word "filter," which is commonly used by the signal and image processing community to denote an "operator." Although the class of increasing transformations is closed under composition, the class of idempotent transformations is not. The following proposition gives a sufficient condition on the sequence of structuring element mappings $\{\theta_i\}$ for the SV alternating sequential filter to be a morphological filter.

Proposition 2:

(a) For every structuring element mapping θ, the SV alternating filter SVAF_θ is a morphological filter.

(b) If θ_i is θ_{i-1}-open (i.e., $\Gamma_{\theta_{i-1}}(\theta_i(z)) = \theta_i(z), \forall\, z \in \xi$), for $2 \le i \le N$, then the SV alternating sequential filter of order N, SVASF_N is a morphological filter.

In the translation-invariant case, the sequence of structuring element mappings is usually chosen to be $\theta_i(z) = (B_i)_z = B_i + z$, where $B_i = B \oplus B \oplus \cdots \oplus B$ (i times) and $B \in \mathcal{P}(\xi)$ [8]. Then, we have $([(i+1)B]_z \ominus iB) \oplus iB = [((i+1)B \ominus iB) \oplus iB]_z = [(i+1)B]_z$; that is, θ_{i+1} is θ_i open. Hence, the condition of Proposition 2 is satisfied in the translation-invariant case. Since for a special choice of the structuring element mapping θ, the SVASF reduces to the translation-invariant ASF, the class of SVASFs is still the subset of smoothing morphological filters which best preserve the crucial structure of input images in the least mean difference sense [8].

2) Simulations: As in the translation-invariant case, SV mathematical morphology theory is not constructive, in the sense that it does not build a systematic algorithm to find the "optimal" structuring element at each point of the image. The choice of the structuring element mapping obviously depends on the considered application.

We propose a general selection rule for image restoration. We assume that the noise model degradation is characterized by the germ-grain model given by (24) and (25). In translation-

[3]Often, the sequence of germs $\{x_{i,n}, n = 1,2,\ldots\}$ is distributed according to a Poisson point process. In this case, the germ-grain model is known as the Boolean model [9], [50], [51].

invariant morphology, *a priori* knowledge of the noise model leads to the selection of a structuring element of size larger than the largest noise-grain [8]. This approach ensures that the noise is eliminated from the image. However, the geometric and topological structure of the restored image is degraded during the restoration process. Denoising should be performed so that the noise is reduced sufficiently and the geometric and topological characteristics of the image are preserved. This can be achieved by spatially varying the structuring element depending on the local properties at each pixel in the image. The idea of the proposed algorithm is to use, at each pixel, a structuring element of size slightly bigger than the size of the noise-grain at that point. The mappings θ_i of the SVASF_N are selected as shown in the equation at the bottom of the page, where $z \in \xi$, S is the 3×3 square structuring element and $i = 1, 2, \ldots, N$. Observe that the above definition of the θ_is does not imply that these mappings are equal, since the noise is reduced as the iterations increase. For instance, assume that at the first iteration, a point z is detected as the center of a noise grain $C(z)$. So, $\theta_1(z) = C(z) \oplus S$. Assume further that the latter noise-grain is small enough so that it has been removed by the filter $\Phi_{\theta_1}\Gamma_{\theta_1}$. Hence, at the second iteration, no noise-grain is detected at point z and thus $\theta_2(z) = \emptyset$, i.e., the point z is not filtered at the second iteration. Moreover, observe that the constructed θ_is do not satisfy Proposition 2 and thus the SVASF_N, for $N \geq 2$, is not idempotent. The detection of the presence of a noise-grain $C(z)$ centered at the pixel z is determined by selecting the largest possible grain C in the germ-grain model given by (24) and (25), which is present or absent in the degraded image (i.e., $C + \{z\} \subseteq Y$ or $C + \{z\} \subseteq Y^c$) [8].

The performance of the algorithm is measured by the signal-to-noise ratio (SNR). Let X_o denote the original image of size $L \times C$ and X_r the restored (denoised) image. The SNR is defined by

$$\mathrm{SNR} = \frac{\sum_{i=1}^{L}\sum_{j=1}^{C} |X_o(i,j)|^2}{\sum_{i=1}^{L}\sum_{j=1}^{C} |(X_o - X_r)(i,j)|^2}.$$

Consider the binary image X depicted in Fig. 1(a). The degraded binary image Y, obtained by using (24) and (25), with $C_{i,n}$, $i = 1, 2$ formed by the overlapping of square structuring elements distributed according to a Bernouilli process, is depicted in Fig. 1(b). Fig. 1(c) [respectively, Fig. 1(d)] shows the output image of the AF using the rhombus structuring element in [43] (respectively, 3×3 square structuring element) dilated eight times. A slight improvement is obtained by the use of an ASF of order 8 using the rhombus structuring element (respectively, 3×3 square structuring element) in Fig. 1(e) [respectively, Fig. 1(f)]. Although most of the noise is removed by the ASF, the original image is highly smoothed and its original topology is lost. We immediately see the drastic improvement of the SVAF and SVASF over their translation-invariant counterparts in Fig. 1(g) and (h), respectively. The SVASF removes the noise while preserving the edges and the geometric structure of the image. The SNR of the different experiments are provided below their corresponding images. The SVASF achieves a SNR 80-dB higher than its invariant homologue.

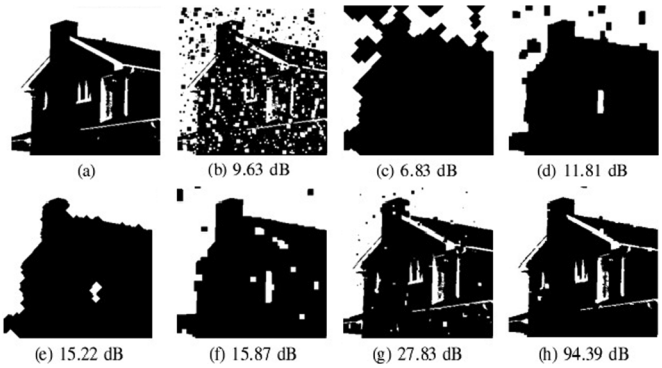

Fig. 1. Denoising of a binary image using morphological filters and SNR comparison. (a) Original binary image. (b) Degraded image by a germ-grain noise model. (c) AF using the rhombus SE dilated eight times. (d) AF using a 3×3 square SE dilated eight times. (e) ASF_8 using the rhombus SE. (f) ASF_8 using a 3×3 square SE. (g) SVAF. (h) SVASF_3.

The simulation results obtained illustrate that, given an image degraded by noise characterized by the germ-grain model, even if one were to select the optimal parametrization [8] and the optimal structuring element [38] for the translation-invariant AF and ASF morphological filters, the results would be inferior to those obtained by using SV morphological filters (see [8, Fig. 3]).

B. Adaptive Median Filter

1) Theoretical Aspects: Consider $\xi = \mathbb{Z}^2$. Let θ be a mapping from ξ into $\mathcal{P}(\xi)$ such that $y \in \theta(y)$ and $|\theta(y)| = \sum_{(i,j)\in\mathbb{Z}^2}[\theta(y)](i,j) = n$ is odd, for every $y \in \xi$. The median $med(X, \theta)$ of X with respect to the adaptive window θ is given by

$$\mathrm{med}(X, \theta) = \left\{ y \in \xi : |X \cap \theta(y)| \geq \frac{n+1}{2} \right\}. \qquad (28)$$

It is easy to show that the median filter is a self-dual $\mathcal{C}$-operator, i.e., it is a $\mathcal{C}$-operator such that it is its own dual. Therefore, it can

$$\theta_i(z) = \begin{cases} -C(z) \oplus S, & \text{if } z \text{ is detected as the center of a noise-grain } C(z) \text{ at iteration } i \\ -\emptyset, & \text{otherwise} \end{cases}$$

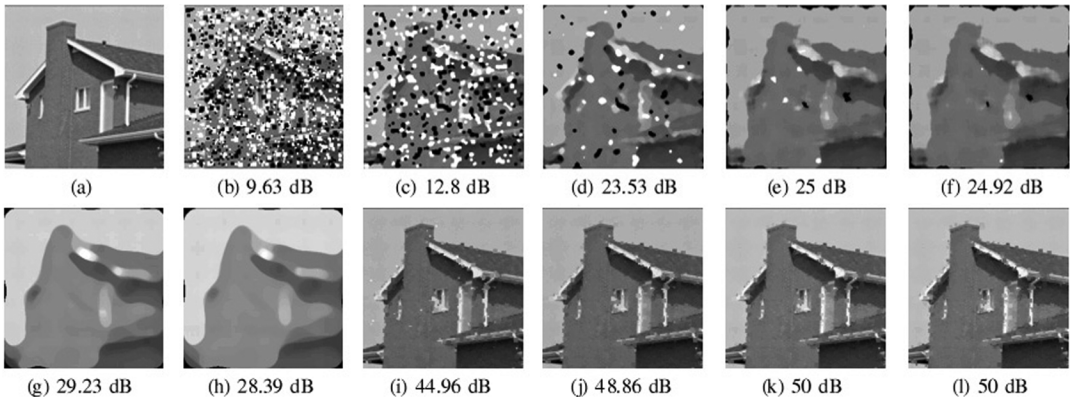

Fig. 2. Denoising using median filters and SNR comparison: (a) Original grayscale image. (b) Image degraded by a germ-grain model. (c) Eight iterations of median filtering by a fixed 3×3 window. (d) Eight iterations of median filtering by a fixed 5×5 window. (e) Median filtering by a fixed 17×17 window. (f) Median filtering by a fixed 19×19 window. (g) Alternating sequential median filter ASMF_8 of size eight using initial window of size 3×3 incremented by two at each iteration. (h) Alternating sequential median filter ASMF_8 using initial window of size 5×5 incremented by two at each iteration. (i) SV median filtering with adaptive window size corresponding to the germ grain size incremented by one. (j) SV median filtering with adaptive window size corresponding to the germ-grain size incremented by two. (k) Second iteration of SV median filtering with adaptive window size corresponding to the germ-grain size incremented by one. (l) Second iteration of SV median filtering with adaptive window size corresponding to the germ-grain size incremented by two.

be shown from the definition of the kernel and from Theorem 1 that

$$\text{med}(X,\theta) = \bigcup_{\lambda \in \mathcal{A}} \mathcal{E}_\lambda(X) = \bigcap_{\lambda \in \mathcal{A}} \mathcal{D}_\lambda(X) \tag{29}$$

where $\lambda : \xi \to \mathcal{P}(\xi)$ and $\lambda \in \mathcal{A}$ if and only if $\lambda(y)$ is any subset of $\theta(y)$ of cardinality $(n+1)/2$.

Equation (29) establishes the relation between the adaptive median filter and the basic SV morphological filters, i.e., SV erosion and SV dilation. The implication of (29) are profound because they enable us to express the adaptive median filter via a closed formula involving only unions and intersections of sets, without requiring any sorting. For small adaptive window sizes, it was shown that the implementation of the median filter via its kernel representation is more attractive than sorting schemes [48].

Although the theory of SV mathematical morphology has been presented for the binary case, its extension to gray-scale is straightforward and follows the steps used to extend translation-invariant binary morphology to translation-invariant gray-scale morphology [37], [42]. Therefore, we will apply adaptive median filtering to gray-scale images.

2) Simulations: The key idea of the implementation of the adaptive median filter is identical to the SVASF. Specifically, the size of the local window at a given point is selected to be slightly larger than the size of the germ-grain at this point. In our simulations, we consider the original image depicted in Fig. 2(a). Its corrupted version by a germ-grain noise model appears in Fig. 2(b).

In the first experiment, we applied the median filter iteratively to the degraded image using a fixed square window of size 3×3. The output image is shown in Fig. 2(c). Notice that since some of the germ-grains have size larger than 3, the median filter using the 3×3 window fails to remove the larger noise structures. We repeat the same experiment using a 5×5 square window. The resulting image is depicted in Fig. 2(d). While the median filter using the 5×5 window removes most of the noise in iteration 8, the output image is more smoothed.

In a second experiment, we applied a Median filter using a fixed square window of size 17×17 [see Fig. 2(e)]. Although more noise has been removed than the iterative median filters in the first experiment, the restored image is overly smoothed. The same experiment is repeated using a square window of size 19×19 [Fig. 2(f)]. The filtered image is cleaner but equally smoothed.

In a third experiment, we applied an alternating sequential median filter (ASMF) of order 8, which is composed of eight median filters of increasing window sizes. The window size is incremented by two at each iteration. Fig. 2(g) shows the result of ASMF using an initial square window of size 3×3. Although the noise-grains are totally removed, the restored image is over smoothed and its features (e.g., windows, edges) are completely lost. We reach the same conclusion if we apply an ASMF using an initial square window of size 5×5 [Fig. 2(h)]. Observe that the largest window of the ASMF with an initial window of size 3×3 (respectively, 5×5) has size 17×17 (respectively, 19×19).

In the last experiment, we applied the SV median filter (SVMF). Fig. 2(i) and (j) is obtained by SV median filtering using, at each point, a local window size equal to the size of the noise-grain, at the same point, incremented by one and two, respectively. The restored images preserve the edges and geometric structure of the noise-free image. Notice that using a local window size equal to the size of the noise-grain incremented by two performs better in terms of noise removal capability, than using a local window of size equal to the size of the noise-grain incremented by one. The reason is that some of the noise-grains overlap and merge to form bigger noise-grains. Therefore, a larger local window size is needed to ensure that these noise-grains are suppressed. However, if the local window size is too large, the median value computed in that window will not provide a good estimate of the noise-free pixel because only pixels in a small neighborhood are strongly correlated. Therefore, there is a trade-off between the noise removal

capability and the accuracy of the estimation. Fig. 2(k) and (l) shows two iterations of the SVMF using a local window size equal to the size of the noise-grain incremented by one and two, respectively. All of the noise has been removed in the second iteration of the SVMF without altering the topological characteristics of the noise-free image. The SNR of the above experiments are provided below their corresponding images in Fig. 2. Notice that the SVAMF achieves a SNR which is 20 dB higher than its translation-invariant counterpart.

IV. Spatially Variant Morphological Skeleton Representation

Let $A \ominus B$, $A \oplus B$, and $A \circ B$ denote the translation-invariant erosion, dilation and opening, respectively, of the set A by the structuring element B [9]. Let $nB = B \oplus B \cdots \oplus B$ (n times).

A. Theoretical Aspects

Consider a sequence of mappings $\{\lambda_n : n \geq 0\}$ from ξ into $\mathcal{P}(\xi)$ such that $z \in \lambda_n(z)$, for every $z \in \xi$, for all n and $\lambda_n(z) \neq \{z\}$, for all n. Consider the sequence of mappings θ_n from ξ into $\mathcal{P}(\xi)$ given by $\theta_{n+1}(z) = \bigcup_{t \in \lambda_n(z)} \theta_n(t) = \mathcal{D}_{\theta'_n}(\lambda_n(z))$ for $n > 0$, $z \in \xi$ and $\theta_0(z) = \{z\}$, for every $z \in \xi$. We define the integer N_X by $N_X = \max\{n : \mathcal{E}_{\theta_n}(X) \neq \emptyset\}$ for a given $X \in \mathcal{P}(\xi)$.

Let $\{\psi_n : n = 0, 1, \ldots, N_X\}$ denote a collection of operators in $\mathcal{O}$ such that

$$\mathcal{E}_{\theta_{n+1}}(X) \subseteq \psi_n(\mathcal{E}_{\theta_{n+1}}(X)) \subseteq \mathcal{E}_{\theta_n}(X) \tag{30}$$

for every $n \in [0, N_X]$, every $X \in \mathcal{P}(\xi)$ and $\psi_n(\emptyset) = \emptyset$, for every $n \in [0, N_X]$.

Definition 2: Consider $X \in \mathcal{P}(\xi)$. The SV morphological skeleton representation $R(X)$ of X is given by

$$R(X) = \{R_0(X), R_1(X), \ldots, R_{N_X}(X)\} \tag{31}$$

where $R_n(X)$ is the SV morphological skeleton representation subset of order n given by

$$R_n(X) = \mathcal{E}_{\theta_n}(X) - \psi_n(\mathcal{E}_{\theta_{n+1}}(X)). \tag{32}$$

Definition 3: The SV morphological skeleton representation of $X \in \mathcal{P}(\xi)$ is invertible if there exists a sequence $\{G_n : n \in [0, N_X]\}$ of operators in $\mathcal{O}$ such that

$$X = \bigcup_{n=0}^{N_X} G_n(R_n(X)). \tag{33}$$

The following theorem establishes a restriction on the choices of the sequences $\{\psi_n : n \in [0, N_X]\}$ as a direct consequence of constraint (30) and establishes the invertibility of $R(X)$ under this restriction.

Theorem 2: If the sequence $\{\psi_n : n \in [0, N_X]\}$ of operators in $\mathcal{O}$ satisfies constraint (30), then

$$\mathcal{E}_{\theta_{n+1}}(X) \subseteq \psi_n(\mathcal{E}_{\theta_{n+1}}(X)) \subseteq \mathcal{E}_{\theta_n}(\Gamma_{\theta_{n+1}}(X)) \tag{34}$$

for $n \in [0, N_X]$ and for every $X \in \mathcal{P}(\xi)$. Moreover, $R(X)$ is invertible and

$$X = R^{-1}(R(X)) = \bigcup_{n=0}^{N_X} \mathcal{D}_{\theta'_n}(R_n(X)). \tag{35}$$

From Theorem 2, we observe that the SV morphological representation of X, $R(X)$, obtained by the sequence of transformations $\{\psi_n : n \in [0, N_X]\}$ which satisfy restriction (30), decomposes into a sequence of $N_X + 1$ subsets $\{R_n(X) : n \in [0, N_X]\}$ which uniquely characterizes X, thereby allowing for a SV morphological representation which permits the exact reconstruction of X. In the remainder of this section, we shall investigate some properties of $R(X)$.

The following proposition shows that the resulting morphological image representation subsets $R_N(X)$, for $n = 0, 1, \ldots, N_X$, are disjoint and anti-extensive.

Proposition 3: We have

$$R_{n_1}(X) \cap R_{n_2}(X) = \emptyset, \text{ for } n_1 \neq n_2 \tag{36}$$

$$R_n(X) \subseteq X, \text{ for } n \in [0, N_X]. \tag{37}$$

In the following proposition we show that, under a certain condition on the mappings $\{\lambda_n : n \in \mathbb{N}\}$, a repeated application of the transformation $R(\bullet)$ does not influence the image representation.

Proposition 4: If

$$\lambda_n(z) \subseteq \lambda_0(z), \text{ for every } z \in \xi \text{ and for } n \in [0, N_X] \tag{38}$$

then

$$R(R_n(X)) = \{R_n(X)\}, \text{ for } n \in [0, N_X]. \tag{39}$$

When condition (38) is not satisfied, the repeated application of $R(\bullet)$ may result in a further reduction of the total cardinality of the representation. This is a desirable result in many applications of interest (e.g., image coding [52], [53]).

1) Example (Generalized Morphological Skeleton [3]): The following example is an important special case of the general SV morphological image representation $R(X)$. Consider

$$\psi_n(X) = \mathcal{D}_{\lambda'_n}(X), \quad n = 0, 1, \ldots, N_X, \ X \in \mathcal{P}(E). \tag{40}$$

The following proposition shows that the above sequence ψ_n satisfies constraint (34).

Proposition 5:

$$\mathcal{E}_{\theta_{n+1}}(X) \subseteq \mathcal{D}_{\lambda_n'}(\mathcal{E}_{\theta_{n+1}}(X)) \subseteq \mathcal{E}_{\theta_n}(\Gamma_{\theta_{n+1}}(X)) \qquad (41)$$

for $n \in \mathbb{N}$ and $X \in \mathcal{P}(\xi)$.

Therefore, the representation $R(X)$, given by (31) and (32), is invertible and the reconstruction formula is given by (35).

B. Algorithmic Analysis

In this section, we develop an algorithm for the implementation of the SV morphological skeleton representation studied above. We compare the SV skeleton representation with the translation-invariant representation. The performance of the morphological skeleton representations is assessed by the number of points, in the image representation, required for exact reconstruction of the original image.

From our perspective, the purpose of morphological skeleton representations is coding, compression and storage. In a communication framework, our goal is to minimize the average code length of the compressed binary image. It has been shown that efficient encoding of the skeleton representation using run-length type codes can be used to provide an efficient compression routine for binary images [43]. This approach relies on the sparse representation of skeletons to efficiently encode long run-lengths corresponding to pixels that do not lie in the skeleton. Therefore, it is not surprising that investigators have determined that lower cardinality skeleton representations yield superior compression ratios [43]. Our goal is thus to minimize the cardinality of the source image under the constraint of lossless compression. For the purpose of this presentation, we assume the channel to be noiseless. Therefore, the receiver will be able to reconstruct the original image perfectly without error.

The optimal SE, in the sense of minimizing the cardinality of the morphological skeleton representation, would be the image itself. The translation-invariant and SV morphological skeleton representations would be identical and consist of one point. However, this is a trivial solution since it is impractical and assumes that the image to be transmitted by the sender is already known by the receiver and is stored in its library. We will assume a fixed library of structuring elements at the encoder and decoder and construct the optimal SV structuring element mapping to minimize the cardinality of the morphological skeleton representation. The idea of the proposed algorithm is similar to the matching pursuit algorithm [54]. The matching-pursuit algorithm adaptively decomposes a signal into waveforms that are the dilations, translations, and modulations of a single function; thus, providing an interpretation of the signal structure. In the proposed algorithm, let X denote the original image and B a fixed structuring element. Table I describes a universal algorithm to construct the optimal structuring element mapping for the SV morphological skeleton representation. The algorithm is an iterative process. At each iteration, the algorithm selects the center of the dilated structuring element nB that maximally intersects the image, for some integer n. The union of these center points constitutes the SV morphological skeleton representation. The exact reconstruction of the original image is guaranteed given the set of center points and their corresponding integer n.

TABLE I
UNIVERSAL ALGORITHM TO CONSTRUCT THE OPTIMAL STRUCTURING ELEMENT MAPPING FOR THE SV-MORPHOLOGICAL SKELETON REPRESENTATION

1. Choose $N_0 = \max\{n : X \ominus nB \neq \emptyset\}$.
2. Let $X_e = X \ominus N_0 B$.
3. Choose $z_0 \in X_e$ such that $|\{z_0\} \oplus N_0 B|$ is maximal.
4. Let $X' = X - (\{z_0\} \oplus N_0 B)$.
5. Store the value of z_0 and N_0.
6. Let $M_{N_0} = 0; k = 0;$
7. While $(X' \neq \emptyset)$ do the following:
   - *a.* $M = 0; N = N_0; k = k + 1;$
   - *b.* While$(|NB| > M \;\&\; N \geq 0)$
     - $N = N - 1$
     - Let $X_e = X \ominus NB$
     - Choose $z_N \in X_e$ such that $|(\{z_N\} \oplus NB) \cap X'|$ is maximal
     - Let $M_N = |(\{z_N\} \oplus NB) \cap X'|$
     - $M = \max_{n=N_0 \cdots N} M_n$
     - Temporarily store z_N
   - *c.* Store z_k and $N_k : |(\{z_k\} \oplus N_k B) \cap X'| = M$
   - *d.* Empty the temporarily stored z_N's
   - *e.* Let $X' = X' - \{z_k\} \oplus N_k B$
8. The SV morphological skeleton representation is then given by $R(X) = \bigcup_{i=0}^{k} \{z_i\}$.
9. The reconstructed image is $X = \bigcup_{i=0}^{k} \{z_i\} \oplus N_i B$.

(a) (b) 162 points (c) 502 points

Fig. 3. Morphological skeleton representation: (a) Original image. (b) SV morphological skeleton representation (162 points). (c) Translation-invariant morphological skeleton representation (502 points).

It is easy to show that the resulting SV morphological skeleton representation using the proposed algorithm is compact, in the sense that the set $\{(z_i, N_i), i = 0, \ldots, k\}$ is not redundant; i.e., the reconstruction based on any partial subset of the resulting SV morphological skeleton representation would form a strict subset of the original image. It is also interesting to observe that the sets $\{\{z_i\} \oplus N_i B, i = 0, \ldots, k\}$ are not necessarily disjoint. Thus, the optimal morphological skeleton representation is not derived by a decomposition of the original image into nonoverlapping shapes. Instead, overlapping shapes are exploited in order to reduce the number of shapes required to cover the image. This approach allows for a substantial reduction in the cardinality of the morphological skeleton representation. Moreover, as we have seen earlier in the example of the SV skeleton representation of a synthetic image, the resulting SV morphological skeleton representation using the optimal SV structuring elements outlined in the algorithm is identical to the SV erosion using the same structuring element mapping. The SV and translation-invariant morphological skeleton representations are shown in Fig. 3(b) and (c), respectively. The SV morphological skeleton representation has a compression ratio which is more than three times higher

than its translation-invariant counterpart. We shall once again determine the number of parameters needed for representation of the skeleton and ignore the effects of the use of encoding schemes using run-lengths type techniques in computing the storage capacity requirements. If the morphological skeleton representation is used for storage or communication, then we need $162 \times 4 = 648$ parameters to transmit the SV morphological skeleton representation. On the other hand, the total number of parameters required for transmission of the translation-invariant morphological skeleton representation is equal to $502 \times 3 = 1506$. Therefore, the SV morphological skeleton representation has a storage capacity gain that is 2.32 times higher than the translation-invariant morphological skeleton representation.

V. Conclusion

In this paper, we presented a general theory of SV mathematical morphology and showed its enormous potential through two important image processing applications. First, we introduced SV alternating sequential filters and SV median filters for SV morphological denoising of degraded images. Simulation results demonstrated that, not only is the noise removal capability of the SV morphological filters dramatically higher than their translation-invariant counterparts, but also the topological and geometrical structure of the original image are preserved. Second, we extended the translation-invariant morphological skeleton representation to the SV case. We have also developed a universal algorithm for optimal selection of the SV structuring element mapping for skeletonization by minimizing the cardinality of the SV morphological skeleton representation. This approach has been shown to yield a substantial reduction in the cardinality of the SV morphological skeleton representation in comparison to its translation-invariant counterpart. As a result of this investigation, we have complemented the elegant theory of SV mathematical morphology with powerful practical algorithms for image processing applications. The SV morphological framework presented can be applied to many classical image processing problems related to nonlinear filtering. In the future, we plan to further explore the power of the SVMM framework by developing more sophisticated and faster algorithms for non linear filtering in various image processing applications. We also plan to investigate the optimal SV structuring element mapping for morphological image restoration applications by extending the work of Schonfeld [38] for translation-invariant morphological filters. We further plan to explore the robustness of the SV morphological skeleton representation to noise degradation by extending the work of Schonfeld and Goutsias [45] for the translation-invariant morphological skeleton representation. A formal analysis of the optimal structuring element mapping and investigation of the robustness of the morphological structuring element require the use of random set theory [6], [9], [50], [51].

Appendix A
Proof of Propositions

Proof [Proof of Proposition 2]: From Section II-A4, we know that Γ_θ and Φ_θ are increasing operators. Since the class of increasing operators is closed under composition, we conclude that the SVAF_θ and the SVASF_N are increasing.

a) Let us first prove the idempotence of the SVAF. By the anti-extensivity property of Γ_θ, we have

$$\Gamma_\theta[\Phi_\theta(\Gamma_\theta(X))] \subseteq \Phi_\theta(\Gamma_\theta(X))$$

for all $X \in \mathcal{P}(\xi)$. Applying Φ_θ to the above inequality and, since Φ_θ is increasing, we obtain

$$\Phi_\theta\{\Gamma_\theta[\Phi_\theta(\Gamma_\theta(X))]\} \subseteq \Phi_\theta[\Phi_\theta(\Gamma_\theta(X))] = \Phi_\theta(\Gamma_\theta(X))$$

where the last equality follows from the idempotence of Φ_θ. Therefore, we have

$$\mathrm{SVAF}_\theta(\mathrm{SVAF}_\theta) \subseteq \mathrm{SVAF}_\theta. \tag{42}$$

By the extensivity property of Φ_θ, we have

$$\Phi_\theta(\Gamma_\theta(X)) \supseteq \Gamma_\theta(X), \quad \forall\, X \in \mathcal{P}(\xi).$$

Applying Γ_θ to the above inequality and since Γ_θ is increasing, we obtain

$$\Gamma_\theta[\Phi_\theta(\Gamma_\theta(X))] \supseteq \Gamma_\theta(\Gamma_\theta(X)) = \Gamma_\theta(X) \tag{43}$$

where the last equality follows from the idempotence of Γ_θ.

Applying Φ_θ to (43), and since Φ_θ is increasing, we obtain

$$\Phi_\theta[\Gamma_\theta(\Phi_\theta(\Gamma_\theta(X)))] \supseteq \Phi_\theta(\Gamma_\theta(X)), \quad \forall X \in \mathcal{P}(\xi).$$

Therefore, we have

$$\mathrm{SVAF}_\theta(\mathrm{SVAF}_\theta) \supseteq \mathrm{SVAF}_\theta. \tag{44}$$

Using (42) and (44), we establish the idempotence of the SVAF_θ.

b) The idempotence of the SVASF_N follows from the more general result established by Schonfeld and Goutsias in [8, Proposition 1]. All the necessary conditions to apply Proposition [8, Proposition 1] are satisfied. ■

Proof [Proof of Proposition 3]: From (32) and constraint (30), we have

$$R_n(X) \subseteq \mathcal{E}_{\theta_n}(X) - \mathcal{E}_{\theta_{n+1}}(X). \tag{45}$$

Assume that $n_1, n_2 \in [0, N_X]$ are such that $n_1 < n_2$. From the definition of θ_n, we have

$$\mathcal{E}_{\theta_{n_2+1}}(X) \subseteq \mathcal{E}_{\theta_{n_2}}(X) \subseteq \mathcal{E}_{\theta_{n_1}}(X) \subseteq \mathcal{E}_{\theta_{n_1+1}}(X).$$

Therefore, $(\mathcal{E}_{\theta_{n_2}}(X) - \mathcal{E}_{\theta_{n_2+1}}(X)) \cap (\mathcal{E}_{\theta_{n_1}}(X) - \mathcal{E}_{\theta_{n_1+1}}(X)) = \emptyset$. From (45), we obtain $R_{n_2} \cap R_{n_1} = \emptyset$. Equation (37) is a direct consequence of (32) and the fact that $\mathcal{E}_{\theta_n}(X) \subseteq X$.

This completes the proof. ∎

Proof [Proof of Proposition 4]: Let $X \in \mathcal{P}(\xi)$ such that $\mathcal{E}_{\lambda_0}(X) = \emptyset$. From the definition of θ_n and λ_n, we have $\lambda_0(z) \subseteq \theta_1(z)$, for every $z \in \xi$. Therefore, $\mathcal{E}_{\theta_1}(X) \subseteq \mathcal{E}_{\lambda_0}(X) = \emptyset$. From (32) and the fact that $\psi_0(\emptyset) = \emptyset$, we have $R_0(X) = \mathcal{E}_{\theta_0}(X) - \psi_0(\mathcal{E}_{\theta_1}(X)) = \mathcal{E}_{\theta_0}(X) = X$. From the constraint (30) and since $\mathcal{E}_{\theta_1}(X) = \emptyset$, we have $\mathcal{E}_{\theta_n} \subseteq \mathcal{E}_{\theta_1} = \emptyset$. Therefore, from (32), we have $R_n(X) = \emptyset$ for $n \geq 1$. Finally, we see that

$$R(X) = \{X\}. \tag{46}$$

Now, we will show that $R_n(X)$ satisfies $\mathcal{E}_{\lambda_0}(R_n(X)) = \emptyset$. Let us take $y \in R_n(X)$. From (32), we see that $y \in \mathcal{E}_{\theta_n}(X)$ and $y \notin \psi_n(\mathcal{E}_{\theta_{n+1}}(X))$. From constraint (30), we see that $y \notin \mathcal{E}_{\theta_{n+1}}(X) \iff \theta_{n+1}(y) \nsubseteq X$. From the definition of θ_{n+1}, there exists $z \in \lambda_n(y)$ such that $\theta_n(z) \nsubseteq X \iff z \notin \mathcal{E}_{\theta_n}(X) \implies z \notin R_n(X)$. Since $z \in \lambda_n(y)$ and by hypothesis $\lambda_n(y) \subseteq \lambda_0(y)$ for $n \in [0, N_X]$, we have $z \in \lambda_0(y)$. Thus, $\lambda_0(y) \nsubseteq R_n(X)$ for every $y \in R_n(X)$. Consider now, $y \notin R_n(X)$ and consider the set $\lambda_0(y)$. By definition of the mappings λ_n, we have that $y \in \lambda_0(y)$. Since $y \notin R_n(X)$, we conclude that $\lambda_0(y) \nsubseteq R_n(X)$ for every $y \notin R_n(X)$. Thus, $\lambda_0(y) \nsubseteq R_n(X)$ for every $y \in \xi$ or $\mathcal{E}_{\lambda_0}(R_n(X)) = \emptyset$. Finally, by using (46) with $X \to R_n(X)$, we prove (39). ∎

Proof [Proof of Proposition 5]: By the extensivity property of the SV dilation, we have that $\mathcal{E}_{\theta_{n+1}}(X) \subseteq \mathcal{D}_{\lambda'_n}(\mathcal{E}_{\theta_{n+1}}(X)) = \psi_n(\mathcal{E}_{\theta_{n+1}}(X))$. By the extensivity property of SV closing, we have

$$\begin{aligned}\psi_n(\mathcal{E}_{\theta_{n+1}}(X)) &= \mathcal{D}_{\lambda'_n}(\mathcal{E}_{\theta_{n+1}}(X)) \\ &\subseteq \Phi_{\theta'_n}(\mathcal{D}_{\lambda'_n}(\mathcal{E}_{\theta_{n+1}}(X))) \\ &= \mathcal{E}_{\theta_n}(\mathcal{D}_{\theta'_n}(\mathcal{D}_{\lambda'_n}(\mathcal{E}_{\theta_{n+1}}(X))))).\end{aligned} \tag{47}$$

Using (10), we have that $\mathcal{D}_{\theta'_n}(\mathcal{D}_{\lambda'_n}(X)) = \mathcal{D}_{\mathcal{D}_{\lambda_n}(\theta'_n)}(X)$. From the construction of θ_{n+1}, we have that $\theta_{n+1}(z) = \cup_{t \in \lambda_n(z)} \theta_n(t) = \mathcal{D}_{\theta'_n}(\lambda_n(z))$, for $n > 0$ and $z \in \xi$. Therefore

$$\begin{aligned}\theta'_{n+1}(z) &= \{y \in \xi : z \in \theta_{n+1}(y)\} \\ &= \{y \in \xi : z \in \mathcal{D}_{\theta'_n}(\lambda_n(y))\} \\ &= \{y \in \xi : \theta'_n(z) \cap \lambda_n(y) \neq \emptyset\} \\ &= \mathcal{D}_{\lambda_n}(\theta'_n(z)).\end{aligned}$$

Therefore, $\mathcal{D}_{\theta'_n}(\mathcal{D}_{\lambda'_n}(X)) = \mathcal{D}_{\mathcal{D}_{\lambda_n}(\theta'_n)}(X) = \mathcal{D}_{\theta'_{n+1}}(X)$, $X \in \mathcal{P}(\xi)$. Finally, (47) becomes $\psi_n(\mathcal{E}_{\theta_{n+1}}(X)) \subseteq \mathcal{E}_{\theta_n}(\mathcal{D}_{\theta'_{n+1}}(\mathcal{E}_{\theta_{n+1}}(X))) = \mathcal{E}_{\theta_n}(\Gamma_{\theta_{n+1}}(X))$.

Therefore, the sequence $\{\psi_n = \mathcal{D}_{\lambda'_n} : n \in [0, N_X]\}$ satisfies constraint (34) for every $X \in \mathcal{P}(\xi)$. Hence, by Theorem 2, $R(X)$ is invertible and $X = \bigcup_{n=0}^{N_X} \mathcal{D}_{\theta'_n}(R_n(X)) = \bigcup_{n=0}^{N_X} \mathcal{D}_{\theta'_n}(\mathcal{E}_{\theta_n}(X) - \mathcal{D}_{\lambda'_n}(\mathcal{E}_{\theta_{n+1}}(X)))$. ∎

APPENDIX B
PROOF OF THEOREMS

Proof [Proof of Theorem 2]: Since constraint (30) must be satisfied for every $X \in \mathcal{P}(\xi)$, we can choose $X \to \Gamma_{\theta_{n+1}}(X)$. Therefore, we obtain

$$\begin{aligned}\mathcal{E}_{\theta_{n+1}}(\Gamma_{\theta_{n+1}}(X)) &\subseteq \psi_n(\mathcal{E}_{\theta_{n+1}}(\Gamma_{\theta_{n+1}}(X))) \\ &\subseteq \mathcal{E}_{\theta_n}(\Gamma_{\theta_{n+1}}(X))\end{aligned} \tag{48}$$

for $n \in [0, N_X]$. From (12), we observe that $\mathcal{E}_{\theta_{n+1}}(\Gamma_{\theta_{n+1}}(X)) = \Phi_{\theta'_{n+1}}(\mathcal{E}_{\theta_{n+1}}(X))$. From the fact that $\mathcal{E}_{\theta_{n+1}}(X)$ is θ'_{n+1}-closed, we have, using Proposition 1

$$\mathcal{E}_{\theta_{n+1}}(\Gamma_{\theta_{n+1}}(X)) = \mathcal{E}_{\theta_{n+1}}(X). \tag{49}$$

Substituting the above equation into (48), we obtain (34).

From (32), we have

$$\mathcal{E}_{\theta_n}(X) = R_n(X) \cup \psi_n(\mathcal{E}_{\theta_{n+1}}(X)) \tag{50}$$

where ψ_n satisfies restriction (30).

Let $\Upsilon_n = \Gamma_{\theta_n}(X)$. Applying $\mathcal{D}_{\theta'_n}$ to (50) and using (34) and the anti-extensivity of Γ_{θ_n}, we obtain

$$\begin{aligned}\Upsilon_n &= \mathcal{D}_{\theta'_n}(R_n(X)) \cup \mathcal{D}_{\theta'_n}(\psi_n(\mathcal{E}_{\theta_{n+1}}(X))) \\ &\subseteq \mathcal{D}_{\theta'_n}(R_n(X)) \cup \Gamma_{\theta_n}(\Gamma_{\theta_{n+1}}(X)) \\ &\subseteq \mathcal{D}_{\theta'_n}(R_n(X)) \cup \Gamma_{\theta_{n+1}}(X) \\ &= \mathcal{D}_{\theta'_n}(R_n(X)) \cup \Upsilon_{n+1}.\end{aligned} \tag{51}$$

Observe that $\Upsilon_{N_X+1} = \emptyset$ and $\Upsilon_{N_X} = \mathcal{D}_{\theta'_n}(R_n(X))$. By iterating (51) for $n = k, k+1, \ldots, N_X$, we obtain

$$\Upsilon_k \subseteq \bigcup_{n=k}^{N_X} \mathcal{D}_{\theta'_n}(R_n(X))). \tag{52}$$

From (32), we have $R_n(X) \subseteq \mathcal{E}_{\theta_n}(X)$; thus, since the SV dilation is increasing, $\mathcal{D}_{\theta'_n} R_n(X) \subseteq \Gamma_{\theta_n}(X)$, i.e.,

$$\mathcal{D}_{\theta'_n}(R_n(X)) \subseteq \Upsilon_n, \tag{53}$$

for $n = 0, 1, \ldots, N_X$. We observe that θ_{n+1} is θ_n-open. Therefore, from (19), we have $\Gamma_{\theta_{n+1}}(X) \subseteq \Gamma_{\theta_n}(X)$, which results in

$$\Upsilon_{n_2} \subseteq \Upsilon_{n_1} \text{for } n_1 \leq n_2. \tag{54}$$

From (53) and (54), we have

$$\bigcup_{n=k}^{N_X} \mathcal{D}_{\theta'_n}(R_n(X)) \subseteq \Upsilon_k. \tag{55}$$

Equations (52) and (55) prove that

$$\Upsilon_k = \bigcup_{n=k}^{N_X} \mathcal{D}_{\theta'_n}(R_n(X)). \tag{56}$$

Observe that $\Upsilon_0 = \Gamma_{\theta_0}(X) = X$. Therefore, we obtain (35). ■

REFERENCES

[1] E. R. Dougherty and C. R. Giardina, *Morphological Methods in Image Processing*. Englewood Cliffs, NJ: Prentice-Hall, 1988.

[2] R. M. Haralick, S. R. Sternberg, and X. Zhuang, "Image analysis using mathematical morphology," *IEEE Trans. Pattern Anal. Mach. Intell.*, vol. 9, no. 2, pp. 532–550, Apr. 1987.

[3] P. A. Maragos, "A Unified Theory of Translation-Invariant Systems With Applications to Morphological Analysis and Coding of Images," Georgia Inst. Technol., Atlanta, 1985, Ph.D. dissertation.

[4] P. A. Maragos and R. W. Schafer, "Morphological filters—Part I: Their set-theoric analysis and relations to linear shift-invariant filters," *IEEE Trans. Acoust., Speech, Signal Process.*, vol. 35, no. 5, pp. 1153–1169, Oct. 1987.

[5] ——, "Morphological filters—Part II: Their relation to median, order-statistics and stack filters," *IEEE Trans. Acoust., Speech, Signal Process.*, vol. 35, no. 5, pp. 1170–1184, Oct. 1987.

[6] G. Matheron, *Random Sets and Integral Geometry*. New York: Wiley, 1975.

[7] D. Schonfeld, "Optimal Morphological Representation and Restoration of Binary Images: Theory and Applications," John Hopkins Univ., Baltimore, MD, 1990, Ph.D..

[8] D. Schonfeld and J. Goutsias, "Optimal morphological pattern restoration from noisy binary images," *IEEE Trans. Pattern Anal. Mach. Intell.*, vol. 13, no. 1, pp. 14–29, Jan. 1991.

[9] J. Serra, *Image Analysis and Mathematical Morphology*. San Diego, CA: Academic, 1982.

[10] ——, "Introduction to mathematical morphology," *Comput. Vis., Graph., Image Process.*, vol. 35, pp. 283–305, 1986.

[11] ——, *Image Analysis and Mathematical Morphology*. New York: Academic, 1988, vol. 2.

[12] P. Soille and M. Pesaresi, "Advances in mathematical morphology applied to geoscience and remote sensing," *IEEE Trans. Geosci. Remote Sens.*, vol. 40, no. 5, pp. 2042–2055, Sep. 2002.

[13] A. D. Kishore and S. Srinivasan, "A distributed memory architecture for morphological image processing," in *Proc. Int. Conf. Information Technology: Coding and Computing [Computers and Communications]*, Apr. 2003, pp. 536–540.

[14] M. H. Sedaaghi, "Direct implementation of open-closing in morphological filtering," *Electron. Lett.*, vol. 33, no. 30, pp. 198–199, Jan. 1997.

[15] A. C. P. Loui, A. N. Venetsanopoulos, and K. C. Smith, "Flexible architectures for morphological image processing and analysis," *IEEE Trans. Circuits Syst. Video Technol.*, vol. 2, no. 3, pp. 72–83, Mar. 1992.

[16] D. Wang and D. C. He, "A fast implementation of 1-D grayscale morphological filters," *IEEE Trans. Signal Process.*, vol. 42, no. 12, pp. 3377–3386, Dec. 1994.

[17] H. J. A. M. Heijmans, "Gray level morphology," Tech. Rep. AM-R9003, Center Math. Comput. Sci., 1990.

[18] ——, "From binary to gray level morphology," Tech. Rep. AM-R9009, Center Math. Comput. Sci., 1990.

[19] H. J. A. M. Heijmans and C. Ronse, "The algebraic basis of mathematical morphology—I: Dilations and erosions," *Comput. Vis., Graph., Image Process.: Image Understand.*, vol. 50, pp. 245–295, 1990.

[20] ——, "The algebraic basis of mathematical morphology—II: Openings and closings," *Comput. Vis., Graph., Image Process.: Image Understand.*, vol. 54, pp. 74–97, 1992.

[21] G. X. Ritter, J. N. Wilson, and J. L. Davidson, "Image algebra: An overview," *Comput. Vis., Graph., Image Process.*, vol. 49, no. 297-331, 1990.

[22] S. Beucher, J. M. Blosseville, and F. Lenoir, "Traffic spatial measurements using video image processing," in *Proc. SPIE. Intelligent Robots and Computer Vision*, Nov. 1987, vol. 848, pp. 648–655.

[23] J. G. Verly and R. L. Delanoy, "Adaptive mathematical morphology for range imagery," *IEEE Trans. Image Process.*, vol. 2, no. 2, pp. 272–275, Apr. 1993.

[24] C. S. Chen, J. L. Wu, and Y. P. Hung, "Theoretical aspects of vertically invariant gray-level morphological operators and their application on adaptive signal and image filtering," *IEEE Trans. Signal Process.*, vol. 47, no. 4, pp. 1049–1060, Apr. 1999.

[25] ——, "Statistical analysis of space-varying morphological openings with flat structuring elements," *IEEE Trans. Signal Process.*, vol. 44, no. 4, pp. 1010–1014, Apr. 1996.

[26] O. Cuisenaire, "Locally adaptable mathematical morphology using distance transformations," *Pattern Recognit.*, to be published.

[27] C. S. Chen, Y. P. Hung, and J. L. Wu, "Space-varying mathematical morphology for adaptive smoothing of 3d range data," in *Proc. 1st Asia Conf. Computer Vision*, Osaka, Japan, Nov. 1993, pp. 39–42.

[28] I. Masayasu, T. Masayoshi, and N. Akira, "Morphological operations by locally variable structuring elements and their applications to region extraction in ultrasound images," *Syst. Comput. Jpn.*, vol. 34, 2003.

[29] J. B. T. M. Roerdink and H. J. A. M. Heijmans, "Mathematical morphology for structuring elements without translation symmetry," *Signal Process.*, vol. 15, pp. 271–277, 1988.

[30] J. B. T. M. Roerdink, "Group morphology," *Pattern Recognit.*, pp. 877–895, 2000.

[31] F. Y. Shih and V. Gaddipati, "General sweep mathematical morphology," *Pattern Recognit.*, vol. 36, no. 7, pp. 1489–1500, Jul. 2003.

[32] G. Birkhoff, *Lattice Theory*. Providence, RI: Amer. Math. Soc., 1984.

[33] G. J. F. Banon and J. Barrera, "Decomposition of mappings between complete lattices by mathematical morphology, part i: General lattices," *Signal Process.*, vol. 30, pp. 299–327, Feb. 1993.

[34] M. C. Chefchaouni, "Morphological representation of non-linear operators: theory and applications," Univ. Illinois at Chicago, 1993, Ph.D. dissertation.

[35] M. C. Chefchaouni and D. Schonfeld, "Spatially-variant mathematical morphology," in *Proc. IEEE Int. Conf. Image Processing*, 1994, pp. 555–559.

[36] N. Bouaynaya, M. C. Chefchaouni, and D. Schonfeld, "Spatially-Variant Mathematical Morphology: A Geometry-Based Theory," Tech. Rep. MCL-TR-2005-01, Multimedia Communications Lab., Univ. Illinois at Chicago, 2004.

[37] S. R. Sternberg, "Grayscale morphology," *Comput. Vis., Graph., Image Process.*, vol. 35, pp. 333–355, 1986.

[38] D. Schonfeld, "Optimal structuring elements for the morphological pattern restoration of binary images," *IEEE Trans. Pattern Anal. Mach. Intell.*, vol. 16, no. 6, pp. 589–601, Jun. 1994.

[39] E. Podaru and D. Stanomir, "Noise suppression using morphological filters," in *Proc. Int. Symp. Signals, Circuits, Systems*, Jul. 2003, vol. 1, pp. 61–64.

[40] H. J. A. M. Heijmans, "Composing morphological filters," *IEEE Trans. Image Process.*, vol. 6, no. 5, pp. 713–723, May 1997.

[41] J. Saniie and M. A. Mohamed, "Ultrasonic flaw detection based on mathematical morphology," *IEEE Trans. Ultrason., Ferroelect., Freq. Control*, vol. 41, no. 1, pp. 150–160, Jan. 1994.

[42] N. Bouaynaya and D. Schonfeld, "Spatially-variant gray-level morphological signal processing: Theory and applications," presented at the SPIE Visual Communications and Image Processing San Jose, CA, 2006, vol. 6077.

[43] P. A. Maragos and R. W. Schafer, "Morphological skeleton representation and coding of binary images," *IEEE Trans. Acoust., Speech, Signal Process.*, vol. ASSP-34, no. 5, pp. 1228–1244, Oct. 1986.

[44] D. Schonfeld and J. Goutsias, "Morphological representation of discrete and binary images," *IEEE Trans. Signal Process.*, vol. 39, no. 6, pp. 1369–1379, Jun. 1991.

[45] ——, "On the morphological representation of binary images in a noisy environment," *J. Vis. Commun. Image Represent.*, vol. 2, no. 1, pp. 17–30, 1991.

[46] R. Kresch and D. Malah, "Morphological reduction of skeleton redundancy," *Signal Process.*, vol. 38, pp. 143–151, Sep. 1994.

[47] W. Kohler, *Gestalt Psychology*. New York: Liveright, 1970.

[48] P. A. Maragos, "A representation theory for morphological image and signal processing," *IEEE Trans. Pattern Anal. Mach. Intell.*, vol. 11, no. 6, Jun. 1989.

[49] C. Lantuejoul and J. Serra, "M-filters," in *Proc. IEEE Int. Conf. Acoustics, Speech and Signal Processing*, Paris, France, May 1982, pp. 2063–2066.

[50] D. Stoyan, W. S. Kendall, and J. Mecke, *Stochastic Geometry and its Applications*. Berlin, Germany: Wiley, 1987.
[51] J. Serra, "The boolean model and random sets," *Comput. Graph. Image Process.*, vol. 12, pp. 99–126, 1980.
[52] D. Schonfeld and J. Goutsias, "A fast algorithm for the morphological coding of binary images," in *Proc. Int. SPIE Conf. Visual Communications and Image Processing III*, Nov. 1988, vol. 1001, pp. 138–145.
[53] R. Kresch and D. Malah, "Skeleton-based morphological coding of binary images," *IEEE Trans. Image Process.*, vol. 7, no. 10, pp. 1387–1399, Oct. 1998.
[54] S. G. Mallat and Z. Zhang, "Matching pursuits with time-frequency dictionaries," *IEEE Trans. Signal Process.*, vol. 41, no. 12, pp. 3397–3415, Dec. 1993.

Nidhal Bouaynaya received the B.S. degree in electrical engineering and computer science from the Ecole Nationale Supérieure de l'Electronique et de ses Applications (ENSEA), France, the M.S. degree in electrical and computer engineering from the Illinois Institute of Technology, Chicago, in 2002, and the Diplôme d'Etudes Approfondies in signal and image processing from ENSEA in 2003. She is currently pursuing the M.S. degree in mathematics and the Ph.D. degree at the Department of Electrical and Computer Engineering, University of Illinois at Chicago.

Her research interests are in signal, image, and video processing; mathematical morphology; and genomic signal processing.

Ms. Bouaynaya won the Best Student Paper Award in Visual Communication and Image Processing in 2006.

Mohammed Charif-Chefchaouni received the B.S. and M.S. degrees in electrical engineering and computer science from the Ecole Nationale Supérieure de l'Aéronautique et de l'Espace, Toulouse, France, in 1978 and 1980, respectively, and the Ph.D. degree in electrical and computer engineering from the University of Illinois at Chicago in 1993.

From 1980 to 1990, he was a Lecturer of applied mathematrics and control at the Institut des Postes et Télécommunications, Rabat, Morocco. He is currently the Director of the Institut National des Postes et Télécommunications, Rabat. His research interests include image modeling and analysis.

Dan Schonfeld (M'90-SM'05) was born in Westchester, PA, in 1964. He received the B.S. degree in electrical engineering and computer science from the University of California, Berkeley, and the M.S. and Ph.D. degrees in electrical and computer engineering from the Johns Hopkins University, Baltimore, MD, in 1986, 1988, and 1990, respectively.

In 1990, he joined the University of Illinois at Chicago, where he is currently an Associate Professor in the Department of Electrical and Computer Engineering. He has authored over 100 technical papers in various journals and conferences. His current research interests are in signal, image, and video processing; video communications; video retrieval; video networks; image analysis and computer vision; pattern recognition; and genomic signal processing.

Dr. Schonfeld was coauthor of a paper that won the Best Student Paper Award in Visual Communication and Image Processing 2006. He was also coauthor of a paper that was a finalist in the Best Student Paper Award in Image and Video Communication and Processing 2005. He has served as an Associate Editor of the IEEE TRANSACTIONS ON IMAGE PROCESSING (Nonlinear Filtering) as well as an Associate Editor of the IEEE TRANSACTIONS ON SIGNAL PROCESSING (Multidimensional Signal Processing and Multimedia Signal Processing).